Investigation of Temperature-Dependent Relaxation Processes in Polyethylene Films by Covalently Attached Anthryl Probe

Oliver Schurr,[†] Sahori B. Yamaki,[‡] Caihua Wang,[†] Teresa D. Z. Atvars,*[,‡] and Richard G. Weiss*[,†]

Department of Chemistry, Georgetown University, Washington, DC 20057-1227, and Instituto de Química, Caixa Postal 6154, Universidade Estadual de Campinas, Campinas, CEP 13083-970, SP, Brazil

Received January 30, 2003; Revised Manuscript Received March 27, 2003

ABSTRACT: The dependence of several aspects of the fluorescence from 9-anthryl groups, covalently attached by tethers of differing lengths to interior sites of five polyolefinic films whose crystallinities range from 0 to 74%, has been explored between 40 and 400 K. The data are employed to determine microscopically the onsets of various relaxation processes of the polymers, the sensitivity of the probes to changes in their local morphologies, and the distribution of the groups between amorphous and interfacial sites. The results are compared with those from noncovalently attached (doped) 9-methylanthracene molecules. Specifically, the relationship between the lengths of tethers for the 9-anthryl groups, as well as the chemical method by which each tether is attached to the polymer chains, and the ability of the fluorescence from the lumophores to detect the onsets of host relaxation processes are explored. The two attachment methods lead to different distributions of lumophores in the amorphous and interfacial regions of the polymers. Furthermore, very short (one atom; methylene) and very long (12 atoms) tethers allow the 9-anthryl groups to sense changes in the local environments more acutely than a tether of intermediate length (three atoms). The advantages of covalent attachment for this sort of study (specifically, the inability of the probe to diffuse within a film from site-to-site with time) and the limitations of the utility of the data are discussed.

Introduction

A variety of methods, including dielectric and dynamic mechanical analyses,[1−3] NMR spectrometry, positron annihilation,[4] and fluorescence spectroscopies,[5−14] have been employed to study relaxation processes in polyethylene and other polymer materials. These diverse methods provide complementary information that, as a combination, can lead to a static and dynamic picture of a polymer. For instance, the loss modulus of a specific type of chain relaxation can be measured by either dynamic mechanical analyses or dielectric measurements.[1−3] Also, the temperature dependence of fluorescence intensities or decays from lumophores doped into a polymer matrix can be used to follow polymer relaxation processes.[5−16] However, the kinetic description of relaxation processes obtained from dielectric and fluorescence measurements are based on different rheological models.[15,16] In addition, guest molecules can be perfused only into the amorphous domains and interfacial regions (i.e., along the lateral faces of crystallites) of semicrystalline polymers.[10,17] As a result, their luminescence provides only secondary information about changes occurring within the interiors of the crystalline domains.

The distribution of amorphous and interfacial regions[18] within PE films and the distribution of lumophores between these two regions, the only ones where they are able to reside,[17c] are also influenced by polymer crystallinity. These distributions are very important to the detection of morphological changes by monitoring fluorescence spectra of the lumophores. If the mole fraction of lumophores near regions where changes in relaxation processes occur is small, the overall emission intensity will be dominated by regions where there is no change and the overall emission intensity will be nearly constant. However, a large mole fraction of lumophores in one domain type does not ensure a change in the fluorescence signal that correlates with motional changes of nearby polymer chains unless those changes are able to couple well with vibronic and other modes of the excited states of the lumophore. Thus, the ability of singlet excited states of 9-anthryl groups to provide measurable information about micromorphological changes in polyethylene films depends on (1) the magnitude of the change produced by the relaxation, (2) the magnitude of the change reflected in the fluorescence of the affected probe molecules, and (3) the fraction of the population of fluorescing probes that experiences the change. The overall observed emission intensity is a convolution of fluorescence from probes that are and are not experiencing changes in their local environments. In particular, small changes are always observed for relaxation processes at lower temperatures because associated motions are small. The sensitivity of other methods is similarly limited for the same reason.

Several methods are available to dope polyolefinic films with lumophores.[10,19,20] Fluorescence from a specific lumophore, anthracene, has been used previously by us to follow local changes that accompany the onset (on heating) or cessation (on cooling) of various processes that occur in unstretched and stretched low-density polyethylene (PE) films between 15 and 400 K.[13] Plots of the integrated fluorescence intensity in stretched and unstretched low-density polyethylene films vs temperature exhibited slope changes near the transition temperatures for relaxation processes identified by other

[†] Georgetown University.
[‡] Universidade Estadual de Campinas.
* Corresponding authors: e-mail weissr@georgetown.edu or tatvars@iqm.unicamp.br.

10.1021/ma034130e CCC: $25.00
Published on Web 04/18/2003

Scheme 1. Protocols for Covalent Attachment of 9-Anthryl (An) Groups to PE Chains; R = $AnCH_2-$ (2) and $An(CH_2)_{10}-$ (3)[11,13,24,27]

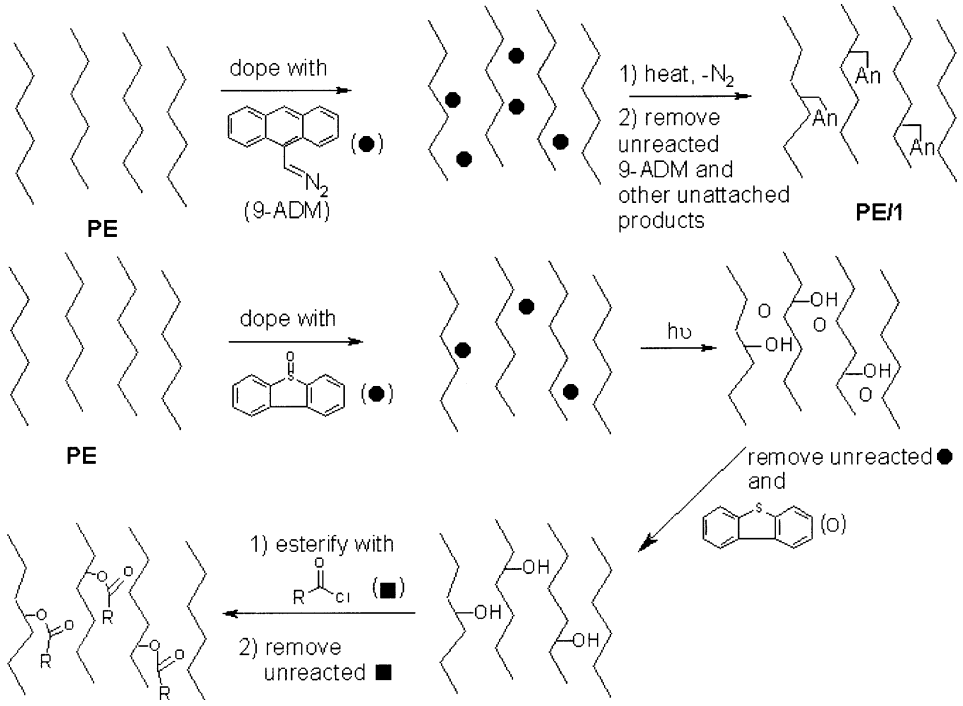

methods.[13] Although these transition temperatures were not dependent on film stretching, the associated slope changes were more pronounced for the stretched films, perhaps as a consequence of the translocations of anthracene molecules from amorphous to interfacial regions that accompany stretching.[13] In addition, fluorescence from 9-anthrylmethyl groups covalently attached to stretched low- and high-density PE films is known to be influenced strongly by cooperative motions of the polymer chains.[11] Because of their inability to diffuse with time or temperature and their very short fluorescence lifetimes (ca. 5 ns in liquid alkanes[21,22]), excited singlet states of attached 9-anthryl groups report only changes occurring near their local environment. In principle, these changes may be perceived differently by one probe in different PE films because each has somewhat different degrees of crystallinity, frequencies of chain branching and chain lengths, degrees of unsaturation, etc.

Covalent attachment of luminescent groups to polymer chains eliminates their large-scale translational diffusion and, thereby, simplifies interpretation of photophysical measurements.[11,23−26] We have developed several methods to attach lumophores selectively to polymer chains in preformed films[11,13,27] and have compared their photophysical properties to those of films containing the same lumophoric groups that are not covalently attached to chains.

The lowest transition temperature that has been identified for a chain relaxation process in polyethylene (PE), T_γ = 120−150 K (the so-called γ-relaxation[28,29]), is attributed to the onset (on heating) or cessation (on cooling) of small segmental motions of polymer chains in the amorphous region[29,30] or with motions of folded chains in interfacial regions.[30] The source of the relaxation process whose transition temperature can be between 195 and 280 K has been ascribed by some authors to the glass transition[31,32] and by others[33−35] to β-relaxations (i.e., motions of short side chains at lamellar[29,36,37] interfaces in the lower temperatures of the range and to main chain motions[31,32] at higher temperatures); we favor the latter assignment. The nature of the α-relaxation ($T_\alpha \approx$ 300−350 K[38]) is also somewhat uncertain; it is thought to involve either reorientational motions in the crystalline domains[39−43] or shear of lamellar surfaces and, hence, amorphous domain deformations,[44,45] since it does not occur in completely amorphous PE.[46−49]

Here, we report the temperature dependence (between 40 and 400 K) of the steady-state fluorescence spectra from 9-anthryl groups that are covalently attached through a methylene group (**1**) or two ω-alkanoyloxy tethers of different lengths (**2** and **3**) to polymer chains at interior sites within several unstretched polyethylene films (Scheme 1). These data are compared with the temperature-dependent changes of fluorescence intensity from doped (i.e., noncovalently attached) anthracene molecules in a low-density polyethylene film.[13] In this way, the relationship between changes in the fluorescence spectra and either the orientation or proximity of parent chains to attached lumophores can be explored, and the influences of diffusion and possible loss of reporter groups (especially at higher temperatures) on the fluorescent properties can be assessed. Specifically, we examine (1) the extent to which fluorescence from the probes senses and reports changes in the dynamics associated with nearby polymer chains, (2) how the lengths of the three linking groups affect the temperature dependence of the fluorescence from the 9-anthryl probes, (3) the correlation between the temperatures at which abrupt changes in the fluorescence data are noted and at which transitions of polyethylene relaxation processes are known from other techniques (e.g., differential scanning calorimetry (DSC)), and (4) the probe concentration ranges above which radiative energy transfer partially masks the local events.

Table 1. Crystallinities (χ), Glass Transition Temperatures (T_g), Melting Temperatures of Crystalline Components (T_m), Thicknesses, and Lumophore Type and Concentration of PE Films Employed

film type	χ (%)[a]	T_g (K)[b]	T_m (K)[b]	thickness (μm)	lumophore type[c]	lumophore concn (mol/kg)[d]
Nordel	0	218		475		
					1	1.1×10^{-4}
EXACT	37		368	31.8		
					1	3.9×10^{-4}
NDLDPE	46	243[51]	ca. 389, 394[e]	76		
					1	9×10^{-3}
					1	$<10^{-4}$
					2	3.0×10^{-3}
					3	1.0×10^{-3}
LLDPE	50		396	25.4		
					1	4.3×10^{-4}
					2	2.0×10^{-3}
					3	2.0×10^{-3}
EHDPE	74		403	12.7		
					1	5.2×10^{-4}

[a] By X-ray diffraction.[51] [b] From differential scanning calorimetry. [c] See Scheme 1. [d] From UV−vis absorption spectra. [e] A polymer blend; both heat flow maxima in DSC thermograms are reported.

Experimental Section

Materials. Diethyl ether (anhydrous, Fisher) was distilled from Na/benzophenone. All other solvents (HPLC grade) and 9-methylanthracene, mp 81−82 °C (lit. mp 81.4 °C;[50] ACROS, 99%), were used as received. NDLDPE is Sclairfilm from DuPont of Canada, Mississauga, Ontario, Canada. LLDPE (LL-3001.63), EXACT (LL-3132), and EHDPE (HD 7745.0) are films from EXXON Chemical Co., Baytown, TX. Films of Nordel (Nordel IP NDR-3430), from DuPont-Dow Elastomers, Wilmington, DE, were prepared by dissolving the as-received polymer in a refluxing 1/1 (v/v) hexane/chloroform solution for several hours, pouring the hot solution slowly into a 2−3-fold volume excess of stirred methanol to precipitate a white mass that was pressed by hand between sheets of aluminum foil, and removing most of the methanol. The films were placed on a fresh piece of aluminum foil in a desiccator under vacuum overnight to remove the remaining solvent. Some of the physical properties and structural characteristics of these and the other films are summarized in Table 1.[51,52]

Films with covalently attached groups are differentiated by lumophore type; for example, EXACT/**1** is an EXACT-type film containing 9-anthryl groups attached via a methylene tether (i.e., R = $AnCH_2-$ in Scheme 1). The NDLDPE/**1** films are designated *h* when [**1**] = 9×10^{-3} mol/kg and *l* when [**1**] < 10^{-4} mol/kg.

Prior to their derivatization or doping, each of the films, except those of Nordel, was immersed repeatedly in $CHCl_3$ and hexane baths for several hours to remove plasticizers, antioxidants, and other additives. They were derivatized by covalent attachment according to procedures described previously (Scheme 1).[11,27] Doped films were prepared by immersing strips of PE in a 10^{-2} M ether solution of 9-MA for various periods followed by quickly washing the film surfaces with methanol and drying in a N_2 stream; depending on the time of immersion and type of film, doping concentrations of 5×10^{-5}−6.5×10^{-3} mol/kg 9-MA were achieved.

The specific procedure for covalent attachment of lumophore **1** to the Nordel film is described. Small pieces of Nordel film were dipped for ca. 2 s into a freshly prepared 0.2 M ether solution of 9-anthryldiazomethane (9-ADM),[53] mp 62−64 °C (decomp) (lit. mp 63−64 °C (decomp)[53]), introducing a deep orange color throughout; diethyl ether is a very good solvent for these films, and they are dissolved after longer immersion periods. After quickly washing their surfaces with methanol and drying them by wiping with a KIMWIPE, the orange films were flame-sealed individually in Pyrex test tubes that subsequently were immersed in a boiling methanol bath for 2 h to decompose 9-ADM and attach 9-anthrylmethyl groups to the polymer chains.[54] Thereafter, the films were immersed in boiling ethanol for 2 days to remove any unattached dopants; ethanol is a good swelling solvent for these films, but prolonged immersion does not dissolve them. The resultant swollen, colorless films were placed on a piece of aluminum foil and left under a dynamic vacuum for 24 h to remove traces of ethanol. To obtain films with uniform thickness, a derivatized and an underivatized Nordel film were placed between two Teflon sheets with aluminum foil on the outside and pressed in a hydraulic press at 70 °C for 2 min with a force of 5 metric tons.

Following attachment of 9-anthryl groups to the films and removal of the unattached precursor molecules from the films,[11,13,27] the concentrations of attached lumophores were determined from Beer's law by averaging absorbances at 389 nm (Perkin-Elmer Lambda 6 spectrophotometer; underivatized film as reference) collected at five different locations on a film surface and assuming molar extinction coefficients of the attached groups or doped molecules are equal to that of 9-MA in cyclohexane (ϵ = 9700 M^{-1} cm^{-1} [55]).

Instrumentation. Differential scanning calorimetry (DSC) of polymer films was performed in closed aluminum pans on a TA 2910 instrument interfaced to a TA Thermal Analyst 3100 controller at a heating rate of 10 °C/min. The cooling rate was proportional to the local temperature of the DSC chamber and room temperature. Steady-state fluorescence spectra of the films doped with 9-MA were recorded at room temperature in flattened quartz capillaries (i.d. 3 × 7 mm) sealed under nitrogen on a SPEX Fluorolog III fluorometer using a 150 W OSRAM xenon arc lamp for excitation. The excitation and emission slits, 0.5 and 0.25 mm, respectively, correspond to bandwidths of 1.8 and 0.9 nm.

Fluorescence spectra (λ_{ex} = 367 nm; λ_{em} = 385−490 nm at 1 nm intervals) of derivatized films sandwiched between quartz disks were recorded at several temperatures from 40 to 400 K in 10 K steps and subsequently at 350 and 300 K (unless indicated otherwise) under dynamic vacuum ($\sim 10^{-4}$ Torr) in a cryostat using an instrument described previously.[11,56] The emission slit (2 mm) and the excitation slits (0.1/0.9 mm) corresponded to spectral bandwidths of 0.2 and 1.4 nm, respectively. Since sets of spectra from each film were collected without changing instrumental parameters or the position of the film while heating and cooling the sample holder, the intensities can be compared directly.

Fluorescence decay histograms were recorded by the time-correlated single-photon counting method using a FL900 Edinburgh Analytical Instruments counter, 0.33 bar of hydrogen as the flash-lamp gas, and 40 kHz pulsing frequency. Decay histograms (λ_{ex} = 367 nm, λ_{em} = 414, 439, and 464 nm) were collected using a time range of 0−100 ns in 1024 channels at 295 K with samples sealed under nitrogen. They were deconvoluted from the lamp decay profile and fitted to a sum of exponential decays (one decay constant plus a small second component attributed to light scatter) employing software provided by Edinburgh Analytical Instruments.

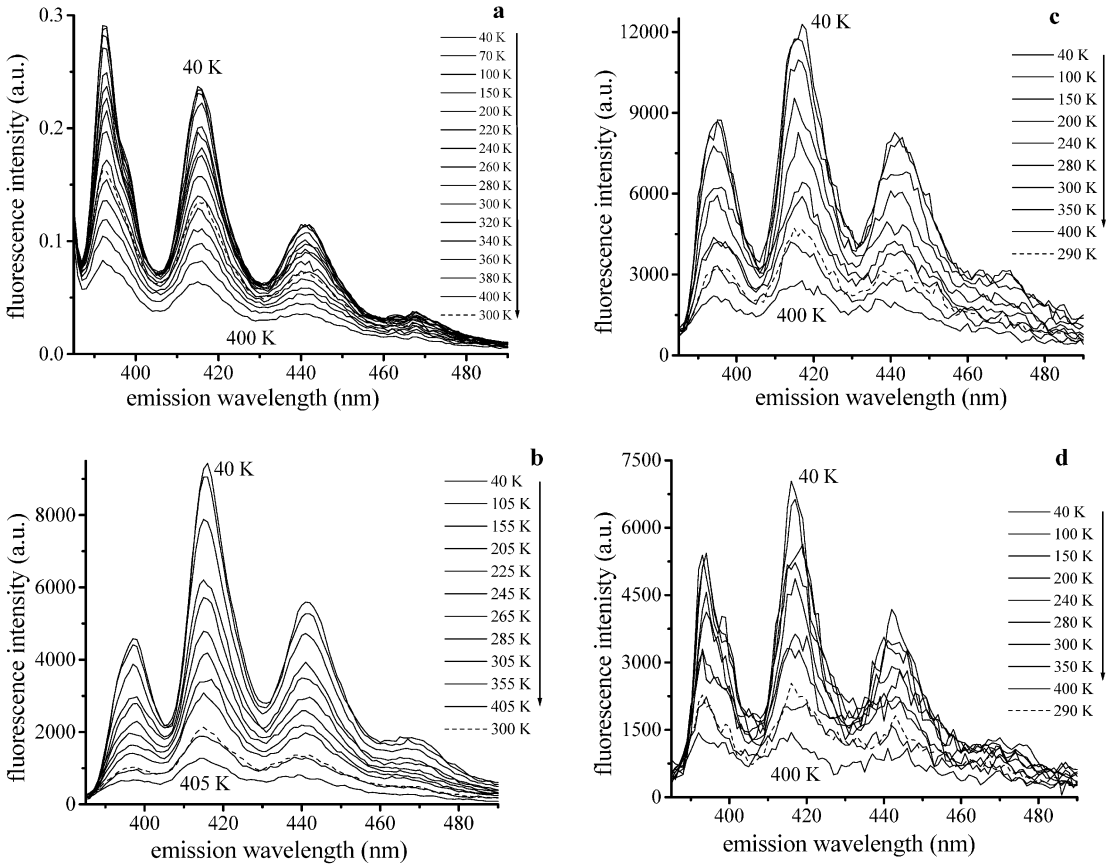

Figure 1. Fluorescence spectra (λ_{ex} 367 nm) of (a) NDLDPE/**1**-*l* (<10^{-4} mol/kg), (b) NDLDPE/**1**-*h* (9×10^{-3} mol/kg), (c) NDLDPE/**2** (3×10^{-3} mol/kg), and (d) NDLDPE/**3** (1×10^{-3} mol/kg). The arrow indicates the order in which the spectra were recorded. Dashed lines indicate the spectra at room temperature after second cooling.

Results

Radiative Energy Transfer in PE Films Doped with 9-MA. The shapes and positions of bands in fluorescence spectra of **1**−**3** in the polyethylene films (Figures 1−3) are very similar to that of 9-MA (Figure 4). Nevertheless, since these spectra can be strongly influence by lumophore concentration, spectral changes and the importance of radiative energy transfer were initially analyzed for 9-MA doped into the same films. When the local concentrations of anthryl groups are high, the small Stokes shift between the excitation and emission spectra allows significant radiative energy transfer[13,57] and consequent reduction of the relative intensity of the 0−0 emission band near 390 nm.[55] The 0−0 emission bands of 9-MA doped in both NDLDPE and LLDPE films (Figure 4a,b) are clearly attenuated, indicating the importance of local (as opposed to bulk) concentrations in the microscopically inhomogeneous films.

The efficiency of radiative energy transfer in polyethylene films is governed by the macroscopic and microscopic implications of Beer's law for reabsorption of emitted radiation and increases with increasing bulk concentrations of anthryl groups, increasing local concentrations, and increasing film thickness. For instance, as the 9-MA concentration in NDLDPE is increased from 5×10^{-5} to 1.2×10^{-3} mol/kg, the band maximum shifts from 391 to 397 nm (due to an inversion of intensities between the 0−0 emission and another vibronic band on its low energy side) and the overall intensity of the overlapping bands decreases (Figure 4a). The loss of 0−0 band intensity occurs despite the low value of the optical density at 389 nm for NDLDPE with 1.2×10^{-3} mol/kg 9-MA, 0.085.

Radiative energy transfer was detectable in emission spectra from 9-MA in LLDPE films (Figure 4b) only at the highest dopant concentration examined, 2×10^{-3} mol/kg (optical density = 0.049 at 389 nm). The difference can be attributed to LLDPE films being only one-third the thickness of NDLDPE films (Table 1); the smaller optical pathway decreases the probability that an emitted photon will be reabsorbed before escaping from LLDPE. In addition, the nature of the crystallites in the LLDPE and NDLDPE films must differ, causing the distribution of their anthryl groups within the amorphous and interfacial regions to differ, also.[17c,18]

At least two types of energy transfer mechanisms among fluorescent groups can occur.[53−55] Were dipole−dipole (Förster) energy transfer responsible for the attenuations, the relative spectral intensities at each wavelength (i.e., the spectral shapes) would have been independent of concentration.[58,59] In addition, the major fluorescence decay component, ~9 ns, in the histograms (λ_{ex} 367 and 389 nm; λ_{em} 414, 439, and 464 nm) of 5×10^{-5}−6.5×10^{-3} mol/kg 9-MA sorbed into NDLDPE films is independent of 9-MA concentration and constitutes >92% of the total emission decay at the lowest concentration and >82% at the highest concentration. These observations are consistent with a radiative energy transfer mechanism but not a dipole−dipole mechanism.

Radiative Energy Transfer in PE Films with Covalently Attached 9-Anthryl Groups. Like the 0−0 emission bands of emission spectra of doped 9-MA

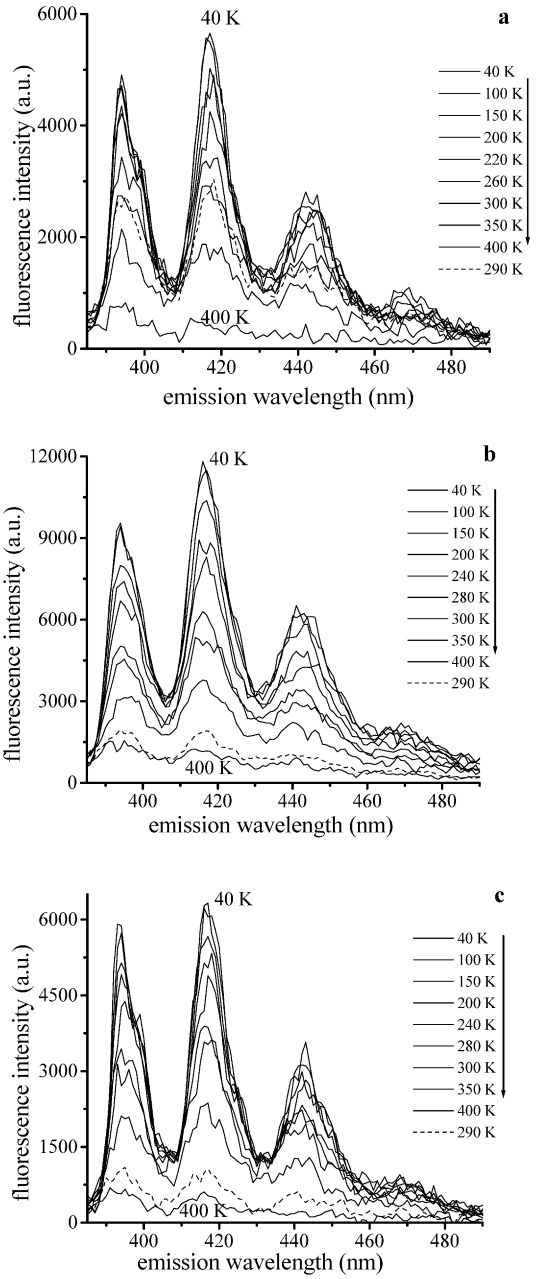

Figure 2. Fluorescence spectra (λ_{ex} 367 nm) of (a) LLDPE/**1** (4.3×10^{-4} mol/kg), (b) LLDPE/**2** (2×10^{-3} mol/kg), and (c) LLDPE/**3** (2×10^{-3} mol/kg). The arrows indicate the order in which the spectra were recorded. Dashed lines indicate the spectra at room temperature after second cooling.

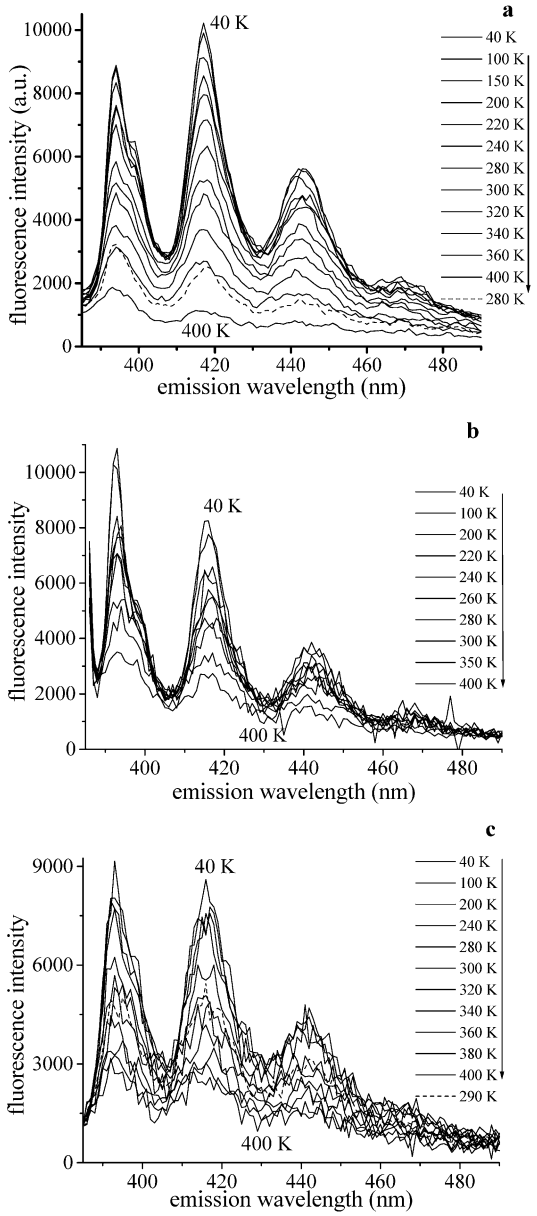

Figure 3. Fluorescence spectra (λ_{ex} 367 nm) of (a) EXACT/**1** (3.9×10^{-4} mol/kg), (b) EHDPE/**1** (5.4×10^{-4} mol/kg), and (c) Nordel/**1** (1.1×10^{-4} mol/kg). The arrows indicate the order in which the spectra were recorded. Dashed lines indicate the spectra at room temperature after second cooling. No spectrum was recorded after cooling EHDPE/**1** from 400 K to room temperature.

molecules, those of covalently attached anthryl groups are concentration dependent in polyethylene films (Figures 1−3). The independence of the fluorescence decay constants on lumophore concentration (vide ante) suggest that Förster energy transfer contributes little to the relatively low intensity of the 0−0 emission band, as well. This conclusion is supported by several experimental observations: (1) lowering the concentration of **1** lumophores from 9×10^{-3} mol/kg (NDLDPE/**1**-*h*) (Figure 1b) to $<10^{-4}$ mol/kg (NDLDPE/**1**-*l*) (Figure 1a) increases the relative intensity of the 0−0 band in emission (Figures 1a,b) to a value expected in the absence of radiative energy transfer; (2) the importance of energy transfer in the NDLDPE films decreases with decreasing lumophore bulk concentrations, independent of the tether type: NDLDPE/**1**-*h* > NDLDPE/**2** ≈ NDLDPE/**3** ≫ NDLDPE/**1**-*l* films (Figure 1); (3) the efficiencies of energy transfer in emission spectra from 9-anthryl groups covalently attached to LLDPE (Figure 2b,c) are lower than those of the analogous NDLDPE films (Figure 1b−d); although the two films are of comparable crystallinity, their thicknesses are very different (vide ante).

The emission spectra of EXACT/**1**, EHDPE/**1**, and Nordel/**1** in Figure 3 indicate little or no radiative energy transfer, albeit for very different reasons, since their anthryl concentrations are similar to that of NDLDPE/**1**-*h* (Figure 1b). The very large film thickness of the Nordel/**1** film, 475 μm, in addition to its being completely amorphous, is offset by its very low local lumophore concentration and more homogeneous distribution of lumophores throughout the entire film volume. The absence of crystalline regions requires that

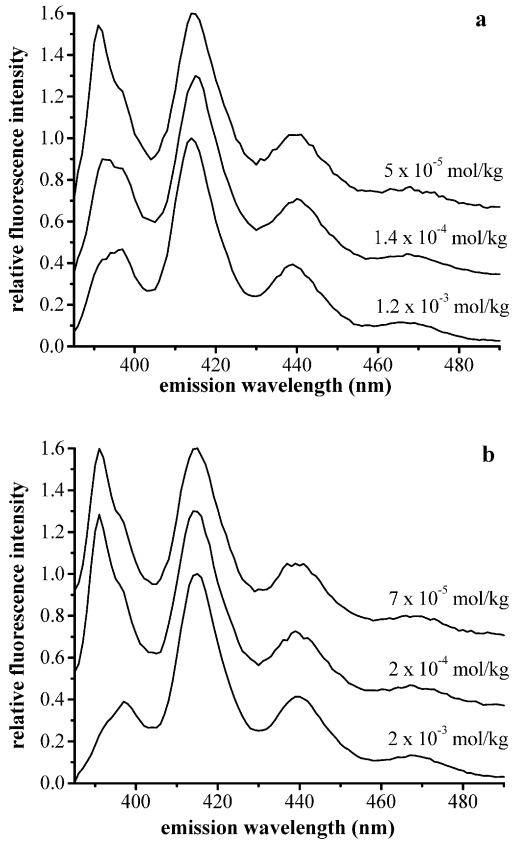

Figure 4. Normalized (and offset) fluorescence spectra (λ_{ex} 367 nm) of (a) NDLDPE and (b) LLDPE films doped with different concentrations of 9-MA.

interfacial regions between amorphous and crystal parts be absent as well (and strongly reduces light scattering). The thinnest of the films, EHDPE/**1** (12.7 μm, Figure 3b), has the highest crystallinity (76%) and bulk lumophore concentration; the local lumophore concentration because the 9-anthryl groups cannot be located inside the crystallites; as a result, the local lumophore concentration in the noncrystalline regions is almost 4 times the value in Table 1. The absence of discernible radiative energy transfer in EHDPE/**1** suggests a very homogeneous distribution of lumophores throughout its noncrystalline domains. Consistent with their similar crystallinities, thicknesses, and lumophore concentrations (Table 1), films of EXACT/**1** (Figure 3a) and LLDPE/**1** (Figure 2a) appear to have similar efficiencies of radiative energy transfer.

In the following sections, the films that lack significant radiative energy transfer will be discussed in detail (i.e., excluding NDLDPE/**1**-*h* for the most part). The first group includes only lumophore **1** (NDLDPE/**1**-*l*, LLDPE/**1**, EXACT/**1**, EHDPE/**1**, and Nordel/**1**) and the second contains **2** (NDLDPE/**2** and LLDPE/**2**) and **3** (NDLDPE/**3** and LLDPE/**3**). NDLDPE/**1**-*h* is discussed superficially.

Determination of the Onset of Morphological Transitions from Integrated Emission Intensities. Earlier investigations have shown that emission intensities from polymer films are influenced by the intrinsic temperature dependence of the lumophore excited states as well as extrinsic properties, such as polymer matrix relaxation processes.[5−16] Although we observe in Figures 1−3 that the emission intensities decrease as expected with increasing temperature, some of the films do not return to their initial room temperature emission

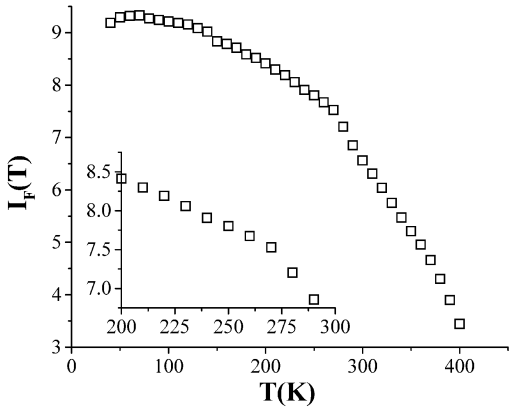

Figure 5. Relative integrated fluorescence (λ_{ex} 367 nm) spectral areas $I_F(T)$ from the NDLDPE/**1**-*l* film as a function of temperature during heating from 40 to 400 K. The insert is an expansion of the 200−300 K data.

intensities upon being cooled from 400 K (dashed spectra in Figures 1−3, except Figures 1a and 3b). Since the lumophores are covalently attached to the polymer chains, the cause cannot be evaporation within the evacuated sample chamber. The noncontinuous changes in emission intensities from temperature-induced physical alterations of polymer morphology do not show a clear trend with film crystallinity (vide infra). However, the degree of crystallinity must influence the distribution of lumophores between amorphous and interfacial regions.[17c,18]

Based on the melting temperatures in Table 1, all of the films except EHDPE are completely melted at 400 K, the highest temperature at which spectra were recorded. The Nordel film has no crystalline parts, and no melting transition was detected by DSC (Figure 1 in Supporting Information). Some physical changes of the melted films, such as thinning due to the pressure applied by the quartz disks that hold them in the cryostat (and corresponding decreases in optical densities), are probably responsible for the lower emission intensities observed after melting. We suspect that the films flow somewhat when melted, with consequent reduction of the thickness, leaving fewer anthryl groups in the excitation beam.

Our data analyses for the relaxation processes of all polymers are based on "integrated fluorescence intensity" at a temperature T, $I_F(T)$. It is the area under an emission spectrum over the wavelength range in Figures 1−3. Each $I_F(T)$ may be compared to others from the same film and temperature-dependent run (during which the sample was not moved and the instrumental parameters were unchanged), but not with $I_F(T)$ values from other films. $I_F(T)$ changes are generally very small below 110 K (Figure 5), where excited singlet states of the 9-anthryl groups return to the ground state almost exclusively through radiative processes,[55] and no relaxation process for polyethylene is expected.

Attempts to extrapolate $I_F(T)$ to the value at 0 K, $I_F(0)$, using various mathematical functions did not yield good fits to the existing data. Therefore, $I_F(40)$ has been taken as the $I_F(0)$ value in all cases except for the Nordel/**1** data. In this film, a more precise $I_F(0)$ was estimated by averaging the $I_F(T)$ between 40 and 160 K, where only random fluctuations in the intensity were observed. $I_F(T)/I_F(0)$ ratios vs temperature are plotted in Figure 6, along with the assignments of observed transition temperatures to polymer relaxation processes from the literature (ranges between bars).[28−45]

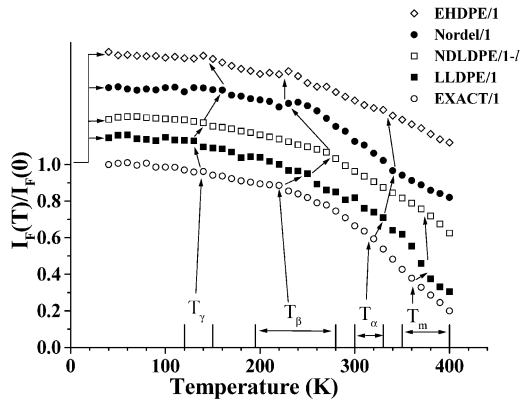

Figure 6. Ratios of relative integrated fluorescence areas, $I_F(T)/I_F(0)$, from films with low lumophore concentrations vs temperature (see Table 1 for details); points for the LLDPE/**1**, NDLDPE/**1**-*l*, Nordel/**1**, and EHDPE/**1** films are vertically offset by 0.15, 0.25, 0.4, and 0.6 units, respectively. Arrows have been drawn at positions of slope changes detected in Arrhenius-type plots of the data (Figure 7) and associated with temperatures for the onset or cessation of the relaxation processes assigned from literature values.[28−45]

The intensity data have also been plotted in Figure 7 according to an Arrhenius-type treatment (eq 1) (vide infra) to aid in the location of onset transition temperatures and to calculate the associated activation energies, E_A, reported in Table 2. The assignments of the onset temperatures in the Arrhenius plots (Figure 7) are somewhat subjective. They are selected as points joining linear regions with significantly different slopes. Points of small vertical offsets between adjacent linear segments of equal slope are not deemed onsets—they may arise from small instrument instabilities—and the complete temperature region is included in the E_A calculation unless a systematic intensity change is observed at such temperatures in several structurally related films. In those cases, it is assumed that an intensity change without slope change is related to the onset of a relaxation process, and the two temperature segments are treated separately.

Linear segments of Arrhenius plots of emission intensities from each sample extend over a wide temperature range which includes transitions of several relaxation processes (as determined using other analytical methods[5−16]). The activation energy of the process commencing at the lowest temperatures within the range is reported, and it is assumed that the other, higher temperature processes cannot be sensed by the fluorescent probe in this range. Using these methods, we have identified three types of activation barriers, but all are not detected in each film: E_{A1} below T_γ, E_{A2} between T_γ and T_β, and E_{A3} above T_β.

$$1 - \frac{I_F(T)}{I_F(0)} = A \exp\left(-\frac{E_A}{RT}\right) \qquad (1)$$

With increasing temperature, the polymer matrix relaxation processes commence successively, and the associated activation energies are expected to be additive; for example, the slope region above T_β should be proportional to the combined activation energy from both the γ- and β-relaxations. However, as shown in Table 2, this comportment is not observed so that the calculated activation energies cannot be assigned to specific morphological relaxation processes. Factors in addition to those responsible for specific relaxation processes must be affecting the efficiency of radiationless decay of the excited singlet states of the alkylanthryl groups.

Changes in the Spectral Shape of the 0−0 Emission Bands with Temperature. Increasing temperature changes the shape of the fluorescence spectra as well as decreasing their intensity; spectral broadening and small red shifts can be detected in Figures 1−3. The full width at half-maximum (fwhm) of the 0−0 emission bands was calculated by fitting the spectrum in the 387−405 nm range (after conversion to wavenumber scale) to two Gaussian peaks using Igor Pro 4.06.[60] They are plotted and compared with the $I_F(T)/I_F(0)$ values in Figures 6−10 of the Supporting Information. Spectral broadening with increasing temperature can result from time-dependent fluctuations of the local lumophore environments that persist for periods at least as long as the excited-state lifetimes. These changes are discontinuous at temperatures corresponding to the onsets of the polymer relaxation processes[61] and should be detectable in the emission spectra if a reasonable fraction of the lumophores is nearby. By contrast, changes in integrated emission intensities report the response of all lumophores, regardless of their specific environments. The two types of data will be discussed together in the following sections.

Films with Lumophore 1 That Lack Discernible Radiative Energy Transfer Processes: NDLDPE/1-l, LLDPE/1, EXACT/1, EHDPE/1, and Nordel/1. As mentioned previously, fluorescence from these films has little radiative or Förster energy transfer, allowing direct comparisons among them (Figure 6). However, their film crystallinities are very different (Table 1). As a result, the apparent concentration of **1** lumophores in the noncrystalline portions is much higher in EHDPE/**1** than in NDLDPE/**1**-*l*, LLDPE/**1**, or EXACT/**1** and is lowest in Nordel/**1.** Thus, we will organize the data analysis beginning with polymers of lowest crystallinity.

As expected, a plot of the relative fluorescence intensities for the Nordel/**1** film shows no changes expected for a melting transition. However, slope changes are observed at 160 K (onset of γ-relaxations), 230 K (onset of β-relaxations), and 340 K. The latter, for which no corresponding change in the DSC thermogram of Nordel (Figures 1 and 15 of Supporting Information) is found, cannot be assigned, in principle, to α-relaxation processes due to the absence of crystallinity in the polymer. It is probably due to a process that is not present in the four semicrystalline PE films.

Discernible slope changes in plots of fluorescence data from the EXACT/**1** film are observed at 130 K (onset of γ-relaxations) and 220 K (onset of β-relaxations), near 310 K (onset of α-relaxations), and around 360 K (onset of melting transition). The evidence for the onset of an α-relaxation in Figures 6 and 7 and the lack thereof in the DSC thermogram of EXACT (Figures 4 and 13 of Supporting Information) demonstrates the utility of the fluorescence measurements as a complementary technique.

The relative fluorescence intensity plot for the NDLDPE/**1**-*l* film has small slope changes around 140 K (onset of γ_2-relaxations), 270 K (onset of the β-relaxations), and near 360 K (onset of melting). The onset of the α-relaxation process in NDLDPE/**1**-*l* is not detected in the Arrhenius-like plot (Figure 7) or the DSC ther-

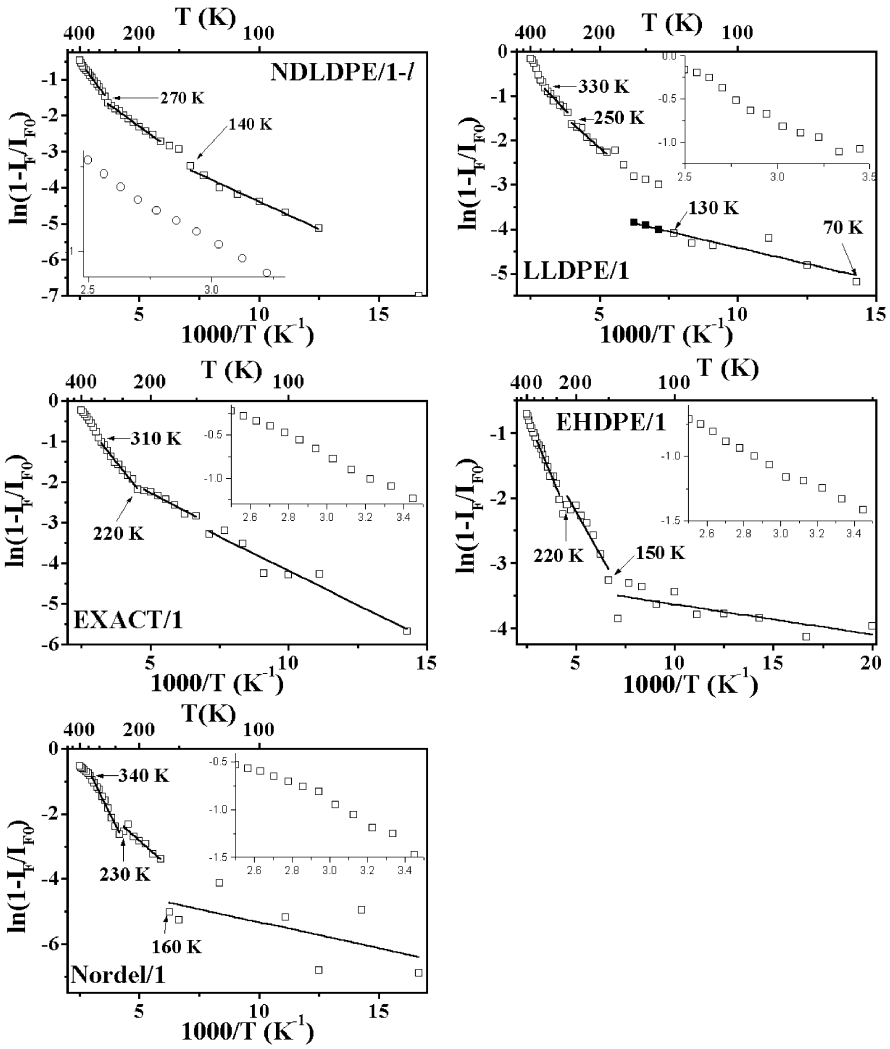

Figure 7. Arrhenius-type plots of the data in Figures 6 with selected linear segments fitted to eq 1; the inserts expand data in the high-temperature region. The three filled points for LLDPE/**1** have been transposed vertically to show the full linear slope range; see text for details.

Table 2. Activation Energies, E_A (kJ/mol), from Arrhenius-Type Plots (Figures 7 and 9) and Corresponding Temperature Ranges, ΔT (K), Grouped According to Lumophore Concentrations[a]

film	ΔT	E_{A1}	ΔT	E_{A2}	ΔT	E_{A3}
Nordel/**1**	60−160 (T_γ)	1.3 ± 0.8	170−230 (T_β)	5.4 ± 0.7	240−330 (T_α)	12.5 ± 0.5
EXACT/**1**	70−140 (T_γ)	2.8 ± 0.3	150−220 (T_β)	3.0 ± 0.2[b]	220−310 (T_α)	7.0 ± 0.2
NDLDPE/**1-*l***	80−140 (T_γ)	2.5 ± 0.1	170−270 (T_β)	4.0 ± 0.1	280−360 (T_m)[c]	7.4 ± 0.2
LLDPE/**1**	70−160 (T_γ)	1.2 ± 0.2	190−250 (T_β)	4.7 ± 0.4	260−330 (T_α)	5.4 ± 0.4
EHDPE/**1**	70−140 (T_γ)	0.4 ± 0.1	150−220 (T_β)	4.4 ± 0.5	230−330 (T_α)	6.1 ± 0.3
NDLDPE/**2**	60−120 (T_γ)	3.6 ± 0.4	140−230 (T_β)	3.8 ± 0.1	240−400[d]	3.9 ± 0.1
NDLDPE/**3**	70−140 (T_γ)	2.4 ± 0.7	150−210 (T_β)	5.1 ± 0.3	230−310 (T_α)	5.8 ± 0.3
LLDPE/**2**	80−160 (T_γ)	4.5 ± 0.4	170−220 (T_β)	3.7 ± 0.2	230−310 (T_α)	5.8 ± 0.2
LLDPE/**3**	60−170 (T_γ)	1.5 ± 0.3	180−250 (T_β)	4.6 ± 0.2	260−320 (T_α)	5.8 ± 0.1

[a] Attributions and transitions from linear slope regions in Figures 6 and 8 are in parentheses. See text for details. Films with **1** are listed in order of increasing crystallinity [b] Region only approximately linear. [c] Onset of melting; see text. [d] No α-onset observed; the high-temperature limit is the highest temperature employed.

mogram of NDLDPE (Figures 2 and 11 of Supporting Information).

Slope changes for the LLDPE/**1** film appear around 160 K (onset of γ-relaxations), 250 K (onset of β-relaxations), 330 K (onset of α-relaxations), and around 370 K (onset of melting). Further evidence for the presence of an α-relaxation in LLDPE is found in its DSC thermogram that shows a small peak around 315 K (Figures 3 and 12 of Supporting Information). The Arrhenius plot for emission from LLDPE/**1** (Figure 7) has one linear range from 70 to 130 K; for reasons discussed above, the data points from 140 to 160 K are made collinear with those in the 70−130 K region, and a single E_A for them is included in Table 2.

Analogous slope changes for the EHDPE/**1** film are observed at 140 K (onset of γ-relaxations) and 220 K (onset of β-relaxations) and a less pronounced α-relaxation at 330 K; again, they are not detectable in the DSC thermogram of EHDPE (Figures 5 and 14 of Supporting Information).

In support of our contention that factors besides bulk crystallinity determine the onset temperatures of re-

laxation processes, we note that the T_β values of EHDPE/**1**, EXACT/**1**, and Nordel/**1** are very similar, despite their wide range of crystallinities. The higher values of LLDPE/**1** and NDLDPE/**1**-*l* (which has the highest T_β among the five films) indicate that their 9-anthryl groups are in less flexible environments than those of EHDPE/**1,** EXACT/**1**, and Nordel/**1**. The T_β values do not appear to depend on the degree of crystallinity or the frequency and type of branches, although the magnitude of the slope change is smaller for the polyethylene with the higher degree of crystallinity.

There is a noticeable change in the integrated emission intensities and fwhm of the 0−0 emission band of the 9-anthryl groups of all polymers, except EHDPE/**1** film (where the change is smaller) near the temperature of the β-relaxation (Figures 6−10 in Supporting Information). In addition, changes are more pronounced in NDLDPE/**1**-*l* (blended material) and Nordel/**1** (amorphous) films. The correspondence of this onset temperature from integrated intensities and fwhm plots of the Nordel/**1**, NDLDPE/**1**-*l*, and LLDPE/**1** films indicate that the same subset of lumophores (in the same local environments) are responsible and that motional averaging, leading to spectral broadening of lumophore emissions, is strongly coupled to the β-relaxation process of the polymer matrix (as well as increasing contributions of lumophore-based nonradiative excited-state relaxations[55]).[61] A similar correspondence between slope changes of integrated intensities and fwhm plots is not found in the EXACT/**1** and EHDPE/**1** films. Its absence may be related in part to the lower emission intensities and signal-to-noise ratios in these films above 300 K. Regardless, it appears that somewhat different populations of lumophores in LLDPE/**1**, EXACT/**1**, and EHDPE/**1** are able to detect the onset of polymer matrix relaxation processes and spectral broadening.

The E_{A1}-like temperature ranges within these five films are similar despite the differences in crystallinity, but the E_{A1} values, 0.4−2.8 kJ/mol, presumably related to the activation energies of γ-relaxation processes, are not and show no clear dependence on crystallinity. The local lumophore environment appears to be more important than bulk crystallinity in determining E_{A1}. Similarly, no consistent trend is found between polymer crystallinity and E_{A2}-like relaxation processes, but the spread of values, 4.0−5.4 kJ/mol, is smaller and, for the most part, the linear temperature ranges are similar. However, if $E_{A2} - E_{A1}$ is the activation energy for β-relaxation processes, their range, from 1.5 (in NDLDPE/**1**-*l*) to ca. 4 kJ/mol (in EHDPE/**1** and Nordel/**1**, the polymers of highest and lowest crystallinity), is quite large. Again, assuming $E_{A3} - E_{A2}$ reflects the activation energy of the α-relaxation processes, their values, from 0.7 (in LLDPE/**1**; within the experimental error limits of zero) to 7.1 kJ/mol (in Nordel/**1**), again follow no discernible pattern with crystallinity. However, we emphasize that the high value in Nordel must be associated with a process other than α-relaxations due to the lack of crystalline regions in this polymer. Although a great deal of information is contained in the Arrhenius-like curves and the activation energies obtained from them, we prefer to use them primarily to help locate the temperatures of onset or cessation transitions of relaxation processes at this point. However, these observations support our contention that factors besides bulk crystallinity (such as branching ratios or lengths of branches) are important in determining the transition temperatures and the associated activation energies. In the Discussion section, the activation energies calculated here and by other methods (for other types of polyethylene) are compared.

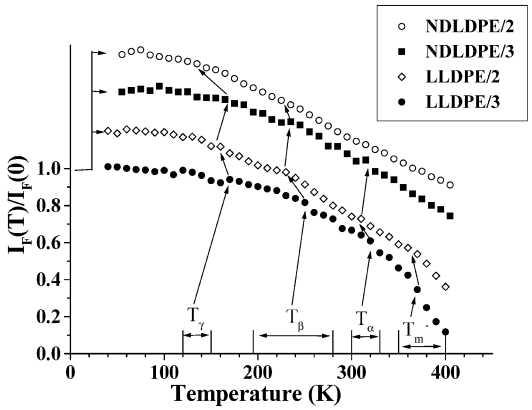

Figure 8. Ratios of relative integrated fluorescence areas, $I_F(T)/I_F(0)$, from films with high lumophore concentrations vs temperature (see Table 1 for details); data for the LLDPE/**2**, NDLDPE/**2**, and NDLDPE/**3** films are vertically offset by 0.2, 0.6, and 0.45 units, respectively. See Figure 6 for an explanation of the slope changes and their assignments.

Films with Lumophores 2 and 3 That Lack Discernible Radiative Energy Transfer Processes. NDLDPE/2, NDLDPE/3, LLDPE/2, and LLDPE/3. As discussed earlier, the lack of radiative energy transfer is a good indicator that the attached 9-anthryl groups are well-separated from each other, and the optical density of the film is low in the region of absorption that overlaps the emission. Furthermore, there are good reasons to believe that the distributions of **2** and **3** between the amorphous and interfacial domains of one film type are virtually the same: (1) their hydroxyl "anchoring sites" are established by a common reagent, DBTO, prior to introduction of the different acyl chloride reagents and covalent attachment (Scheme 1), (2) the ability of the acyl chloride precursors of **2** and **3** to access the hydroxyl groups is controlled primarily by a (common) swelling solvent, and (3) the concentrations of the acyl chlorides are much greater than the concentrations of hydroxyl groups within the films.

The transition temperatures from plots of integrated fluorescence intensity (Figure 8) and the corresponding Arrhenius-like curves (Figure 9) are listed in Table 2. At temperatures above the γ-transition (near 130 K), the Arrhenius-like plot for NDLDPE/**2** is more linear than that of NDLDPE/**3**, despite the relative distribution of lumophores in amorphous and interfacial sites of the two films being similar. This suggests that lumophore **2** does not perceive changes in its local environment as well as lumophore **3**. Regardless, they and the Arrhenius-like plots from LLDPE/**2** and LLDPE/**3** (Figure 9) can be dissected into several linear slope regions. Although several of the E_A values for one polymer film with **2** and **3** as the reporter agree well (and with the values obtained from **1**), others do not. The differences must be related to factors associated with the lengths of the tether groups.

Discussion

Physical Properties of Polyethylene Films. The polyethylene films in Table 1 encompass a very wide

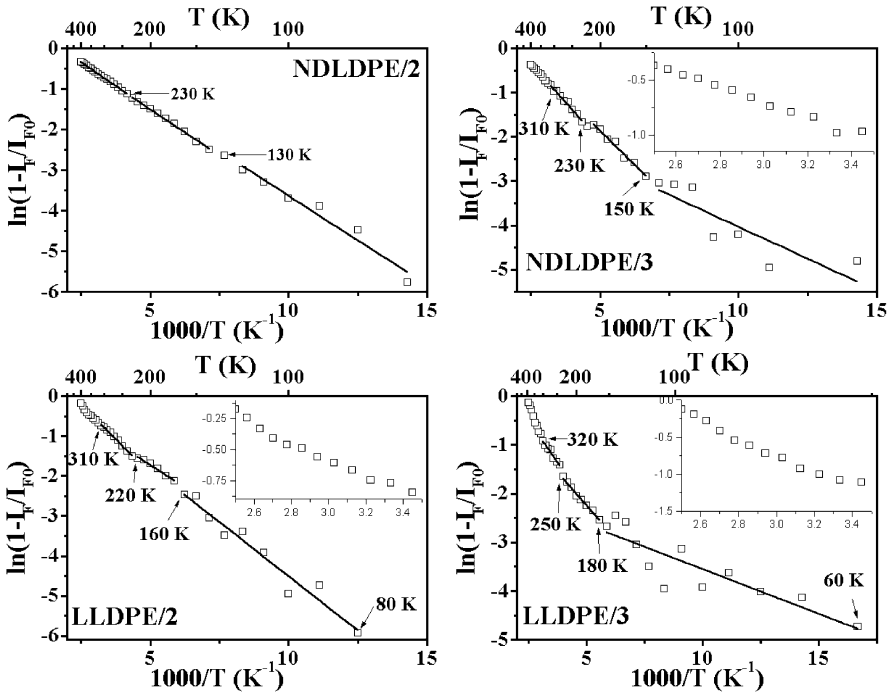

Figure 9. Arrhenius-type plots of the data in Figure 8 with selected linear segments fitted to eq 1; the insets expand data in the high-temperature region.

range of crystallinities[51] (an indicator of the frequency and length of branches,[62,63] the molecular weight, and the sample history[64]). For instance, polyethylenes containing few chain branches usually have higher degrees of crystallinity and higher melting points than polyethylenes with higher branching ratios.[64] In the extreme, at extremely high degrees of branching, polyethylene becomes completely amorphous. Furthermore, polyethylenes with many long chain branches usually have broad molecular weight distributions,[65,66] but the lengths of the branches have little influence on the degree of crystallinity.[67] Thus, on the basis of its lower crystallinity and melting temperature, EXACT has a higher branching ratio than NDLDPE or LLDPE. Although they are comparable in crystallinity, the low-density film NDLDPE should have many short side branches and few long ones[29] while the linear low-density LLDPE has few, but long, branches.[68] The polymer with the highest degree of crystallinity and melting temperature, EHDPE, is expected to contain the fewest branches.

These morphological differences are relevant to our measurements because lightly and highly branched polymers respond to temperature changes somewhat differently at macroscopic and nanoscopic distance scales. Consistent with data from the manufacturer that Nordel is almost completely amorphous,[69] its DSC heating curve (Figure 7 in Supporting Information) gave no evidence of a melting transition. Thus, its fluorescence is from lumophores attached to segments of the macromolecular chains only at "amorphous" sites.

PE Melting Temperatures. Differences between the onset of melting temperatures (T_m) inferred from Figures 6 and 8 and peak melting temperatures measured by DSC (Table 1 and Supporting Information) are expected.[18] In addition, the T_m from fluorescence measurements is less precise because data were collected at 10 K temperature intervals, allowing for absolute errors of at least ±5 K, and the 9-anthryl probes disturb somewhat their local environments. As a result, the locally determined T_m can be depressed by the presence of the probe groups. In addition, the fluorescence intensities are very low at the higher temperatures so that precision of the measurements is lower. Fluorescence changes under these conditions reflect much more the higher mobility of the viscoeleastic medium than the behavior of the crystalline or interface regions. By contrast, DSC measures bulk thermal properties without the necessity of probe groups. In addition, the melting endotherms on heating and crystallization exotherms on cooling for NDLDPE from DSC thermograms are very broad and consist of two components (Figures 2−4 of Supporting Information). The two endothermic peaks observed for LLDPE and EXACT films are attributed to the melting of smaller and larger crystals since one of the corresponding peaks is absent during sequential sample cooling. NDLDPE, the PE for which the endotherm is most complex, is a blend of two components.[18] For these reasons, the T_m values from fluorescence data reported in Table 2 must be interpreted in terms of local rather than bulk changes in chain mobility.

The onset of melting of crystallites is detectable by fluorescence changes in NDLDPE/**1**-*l*, LLDPE/**1**, and EXACT/**1** (Figure 6), albeit by a very small slope change. These observations are reasonable considering the mole fraction of crystallites, the ratio of interfacial area to amorphous volume, the distribution of lumophores between interfacial and amorphous sites in films of lower crystallinities, and the logical assumption that the magnitude of the expected fluorescence intensity changes due to melting of crystallites will be much greater for lumophores in interfacial sites than in amorphous ones. It follows that a mechanistically significant percentage of the lumophores is in interfacial regions in these films and is responsible for the observed small slope changes when crystallites melt.

Influence of Lumophores on Local Polymer Structure. Reported activation energies for the same types of changes in polyethylene as those reported in Table 2 are 1−2 orders of magnitude larger when

monitored by less invasive (but more macroscopic) analytical techniques.[70,71] For instance, the calculated activation energies derived for α-, *β*-, and *γ*- relaxations in polyethylenes from dynamic mechanical measurements are 420, 160−200, and 32 kJ/mol, respectively.[70] Dielectric measurements on slightly chlorinated or oxidized polyethylene films of 22−27% crystallinity provided activation energies of 99−125, 210−245, and 45−50 kJ/mol for α-, *β*-, and *γ*-relaxations, respectively.[71]

Because of the short fluorescence lifetimes of the covalently attached anthryl groups, they are able to sense their local environments only. As a result, any changes in the observed fluorescence emission spectra or integrated intensities can be directly related to local changes in the polymer matrix. By contrast, dielectric or dynamic mechanical spectroscopies (like differential scanning calorimetry) probe the bulk of a polymer sample. The shape, size, and electronic character of the 9-anthryl groups must frustrate isomorphous substitution, disturb their local environments, and lead to attenuation of their sensitivity to changes even in nearby undisturbed regions. The effects must be analogous to those induced by solvent swelling, including increasing the local free volume around the lumophores.[72−75] Film stretching, another means to modify macroscopically polyethylene films, decreases the mean free volume of "voids" and increases the sensitivity of lumophoric groups to changes occurring around them.[23−26,76]

Moreover, fluorescence is a kinetic process whose intensity depends on the degree to which nonradiative processes, that can be strongly linked to movement and location of "solvent" chains in the vicinity of the lumophore, are suppressed. The mobility of the immediate environment increases the efficiency of nonradiative processes. In particular, if a fluorescent group is attached to a polymer segment directly involved with a relaxation mode, polymer mobility and fluorophore deactivation will be strongly correlated events.

Fluorescence Sensitivity to Tether Length and Lumophore Distribution. The sensitivity of 9-anthryl emissions to changes in polymer chain relaxations should depend on tether length. For instance, conformational constraints on the tethers can change the alignment of the 9-anthryl groups with respect to their neighboring polyethylene chains. Moreover, the magnitudes of van der Waals forces between the tethers of **1**−**3** and local polymer chains can affect orientation. The energy of van der Waals interactions between neighboring methylene groups is ∼6.9 kJ/mol.[77] As a result, interactions between the long methylene chain of lumophore **3** and neighboring polymer chains can force alignment of the 9-anthryl group in ways that are not possible with lumophore **2** (or lumophore **1**). The 9-anthryl groups of **3** may be coupled more tightly to the local polymer matrix through an "antenna" (the tether chain) and be able, therefore, to sense smaller motional changes of nearby polymer chains than the lumophores of **1** or **2**.

In one polyethylene film, the fluorescence intensity from **1**, **2**, and **3** may depend differently on temperature because of the disparity of strengths of van der Waals interactions and variations in the alignments between the lumophores and neighboring polyethylene chains. In addition, alkyl tethers whose lengths are similar to the lengths of the branches of the polyethylene chains may plasticize their local environments, increasing chain mobility near the lumophore. Consequently, both the ability of the probes to sense changes in their local environments and the relationship between the temperatures at which those changes occur locally and in the polymer bulk will depend on tether length.

In addition, the relative distributions of 9-anthryl groups between amorphous and interfacial sitesin each film may differ when attachment is via decomposition of ADM (leading to **1**) and by the hydroxylation/esterification method (leading to **2** and **3**) (Scheme 1), but the relative distributions of lumophores **2** and **3** should be very similar. If the differences between the relative populations of lumophores in amorphous and interfacial sites, resulting from the two derivatization methods, are large, **1** may be able to detect some relaxation processes better (and others worse) than **2** and **3** for reasons that have nothing to do with tether length. For instance, lumophores attached primarily to interfacial sites should be able to detect better the onsets of α-relaxations.

In this regard, the absence of a detectable onset for α-relaxations from fluorescence in NDLDPE/**1**-*l* suggests that molecules of ADM (and, therefore, lumophore **1**) reside predominantly in the amorphous regions of NDLDPE. The onsets of α-, *β*-, and *γ*-relaxation processes are discernible in NDLDPE/**3** and, to a lesser extent, in NDLDPE/**2**; a similar difference in sensitivity between **2** and **3** is found in the LLDPE films (Figure 9). On this basis, we conclude that a larger fraction of the **2** and **3** lumophores than the **1** lumophores reside in sites within the interfacial region, and at least some of the sensitivity difference between **2** and **3** is attributable to the degree to which the tether groups allow the excited singlet states of the 9-anthryl groups to couple to their local environments. Both tether length and lumophore location contribute to the ability of the onsets of relaxation processes to be detected via fluorescence changes.

The frequency and type of main-chain branches must also be considered when comparing quantitatively how **2** and **3** perceive their local environments in NDLDPE and LLDPE. Although the detailed nature of the differing interactions are not understood at this time, it is clear that the fluorescence of **2** and **3** responds differently when in polyethylenes of different microstructures; further interpretation will require additional investigations. Consequently, the apparent activation energies in Table 2 cannot be interpreted easily with the information in hand. However, we propose that an "antenna" effect, provided by the long methylene chain of **3**, is the principal reason for its better sensitivity.

When the bulk concentration of lumophore **1** is low, it is able to detect a wide range of relaxation processes in several types of films despite their crystallinity differences (and resulting amorphous/interfacial lumophore distribution differences). It seems reasonable that the short tether of **1**, forcing the 9-anthryl groups to be very near the polymer chain to which they are attached, aids their ability to detect local changes.

Thus, irrespective of the distributions of lumophores between the amorphous and interfacial regions, the least well-coupled 9-anthryl groups to their immediate environment, in lumophore **2**, lack the enforced proximity of 9-anthryl groups of **1** to their polymer chains of attachment and the "antenna" coupling of 9-anthryl groups of **3**. The quantitative differences in sensitivity

among the probes further depend on the frequency and types of branches present in the polymer matrix. For instance, we propose that the best coupling occurs when polymer branches and the tether of **3** are similar in length.

Comparison with Results from Unattached Anthracene Lumophores in Polyethylene Films. Previously, we investigated the temperature dependence on the fluorescence from anthracene molecules doped (i.e., not covalently attached) in a low-density polyethylene film of 47%[78] crystallinity.[13,79] In those experiments, changes associated with the onsets of the α-, β-, and γ-relaxation processes could be discerned, but the probes suffered significant translocations between site types, especially above T_β. The apparent activation energies for the γ- and β-relaxations, 0.4 and 0.6 kJ/mol, respectively, are somewhat smaller than those reported here. More importantly, the calculated energy of the α-process, ca. 10.5 kJ/mol, is larger than reported here because it is a convolution of the actual changes to the lumophore emission efficiency and the loss of probe molecules via sublimation under the dynamic vacuum of the cryostat. Covalent attachment of probes, as in the current study, avoids complications of this sort and also allows spectral changes to be recorded on cooling from the melt; cooling the melted films that were doped with anthracene did not result in an increased fluorescence intensity due to the irreversible loss of lumophores on heating.[13] Clearly, the use of unattached probes limits their utility to the lower temperature regions, and even there, the possibility of transposition of probes between different site types cannot be discounted. Covalently attached lumophores allow quantitative spectroscopic (diagnostic) measurements to be made reproducibly, even at elevated temperatures and under vacuum.

Conclusions

An important feature of this work is that the 9-anthryl probes are covalently attached to polymer chains. This ensures that they continue to reside within the same sites for the duration of the film lifetime, regardless of temperature (below the melting temperature), thus avoiding complications to interpretations of data that attend noncovalently attached, diffusing fluorescent probes. We have explored how fluorescence from the probes is influenced by temperature, crystallinity of the polymer matrix, the length of tethers and the method by which they are attached to polymer chains, and the distribution of the lumophores between amorphous and interfacial regions in the films. The temperature-induced variations in the integrated fluorescence intensities can be correlated with the onsets of relaxation processes of the films provided the fraction of lumophores residing in the vicinity of the motional changes is large. Only that fraction of lumophores in a phase region experiencing a change will be affected by it, although the fluorescence intensity reports the weighted average environment of all lumophores.

The less than optimal coupling between the motions of the polyethylene chains and the photophysical properties of the excited singlet states of the 9-anthryl groups attenuates the response transmitted by the fluorescence. For very different reasons, 9-anthryl groups with short and long tethers are better coupled to their local environments than the tether of intermediate length. Since (1) the coupling with the matrix varies with tether chain length and (2) the fluorescence reports events occurring at the nanoscopic scale from polyethylene environments that are somewhat disturbed by the lumophores, the fluorescence-derived activation energies are much smaller than the values obtained by bulk measurements. However, from knowledge of the parts within the inhomogeneous films where the relaxation processes take place, it is possible to use the fluorescence changes (or lack thereof) to approximate the distribution of lumophores covalently attached within the amorphous and interfacial parts.

By judicious selection of the attachment method and the length of the tether, we have shown that it is possible to modulate both the distribution of the probes and their sensitivity to environmental changes. At this point, the level of control of these factors is not good; further investigations will be required to determine the levels of specificity and sensitivity that can be achieved. In this regard, additional methods of probe attachment would be useful since they may be able to differentiate amorphous and interfacial sites more specifically than the two employed here.

The techniques described here are not a substitute for bulk measurements of the same relaxation processes. They are complementary to them and offer a window into relaxation processes on a much different distance scale and in very different local environments. Although we have concentrated our efforts on undrawn polyethylene films and 9-anthryl groups here, the same methodologies should be applicable to a wide variety of bulk polymers and reporter groups.[27] Future investigations will use these methodologies to compare the changes encountered when films are drawn or modified by high-energy ionizing radiation.

Acknowledgment. The Georgetown group thanks the U.S. National Science Foundation, and the Campinas group thanks FAPESP, MCT, and CNPq (Brazil) for financial support and fellowships. We are grateful to EXXON Chemical Co., Baytown, TX, for EXACT, EHDPE, and LLDPE films, DuPont of Canada, Mississauga, Ontario, Canada, for NDLDPE films, and Dow DuPont Elastomers, Wilmington, DE, for Nordel polymer.

Supporting Information Available: Figures 1−15 of DSC thermograms and relative fluorescence intensities. This material is available free of charge via the Internet at http://pubs.acs.org.

References and Notes

(1) Buerger, D. E.; Boyd, R. H. *Macromolecules* **1989**, *22*, 2699−2705.
(2) Boyd, R. H. *Polymer* **1985**, *26*, 323−347.
(3) Smith, G. D.; Liu, F.; Devereaux, R. W.; Boyd, R. H. *Macromolecules* **1992**, *25*, 703−708.
(4) Dlubek, G.; Lüpke, T.; Stejny, J.; Alam, M. A.; Arnold, M. *Macromolecules* **2000**, *33*, 990−996.
(5) Sommersall, A. C.; Dan, E.; Guillet, J. E. *Macromolecules* **1974**, *7*, 223−244.
(6) Tazuke, S.; Winnik, M. A. In *Photophysical and Photochemical Tools in Polymer Science*; Winnik, M. A., Ed.; D. Riedel: Dordrecht, 1986; pp 15−42.
(7) Winnik, M. A. In *Photophysical and Photochemical Tools in Polymer Science*; Winnik, M. A., Ed.; D. Riedel: Dordrecht, 1986; pp 611−627.
(8) Toynbee, J.; Soutar, I. In *Photophysics of Polymers*; Hoyle, C. E., Torkelson, J. M., Eds.; American Chemical Society: Washington, DC, 1987; Chapter 11.
(9) Christoff, M.; Atvars, T. D. Z. *Macromolecules* **1999**, *32*, 6093−6101.

(10) Atvars, T. D. Z.; Sabadini, E.; Franchetti, S. M. *Eur. Polym. J.* **1993**, *29*, 1259−1264.
(11) Talhavini, M.; Atvars, T. D. Z.; Schurr, O.; Weiss, R. G. *Polymer* **1998**, *39*, 3221−3232. (b) Schurr, O. Ph.D. Thesis, Georgetown University, Washington, DC, 2002.
(12) Vigil, M. R.; Bravo, J.; Atvars, T. D. Z.; Baselga, J. *Macromolecules* **1997**, *30*, 4871−4876.
(13) Talhavini, M.; Atvars, T. D. Z.; Cui, C.-X.; Weiss, R. G. *Polymer* **1996**, *37*, 4365−4374.
(14) Atvars, T. D. Z.; Dorado, A. P.; Pierola, I. F. *Polym. Network Blends* **1997**, *7*, 111−116.
(15) Klopffer, M.-H.; Bobobza, L.; Monnerie, L. *Macromol. Symp.* **1997**, *119*, 119−128.
(16) Klopffer, M.-H.; Bobobza, L.; Monnerie, L. *Polymer* **1998**, *39*, 3445−3449.
(17) Meirovitch, E. *J. Phys. Chem.* **1984**, *88*, 2629−2635. (b) Michl, J.; Thulstrup, E. W. *Spectroscopy with Polarized Light*; VCH: Deerfield Beach, 1986. (c) Phillips, P. J. *Chem. Rev.* **1990**, *90*, 425−436.
(18) Zimerman, O. E.; Cui, C.-X.; Wang, X.; Atvars, T. D. Z.; Weiss, R. G. *Polymer* **1998**, *39*, 1177−1185.
(19) Prado, E. A.; Yamaki, S. B.; Atvars, T. D. Z.; Zimerman, O. E.; Weiss, R. G. *J. Phys. Chem. B* **2000**, *104*, 5905−5914.
(20) Konar, J.; Sen, A. K.; Bhowmick, A. K. *J. Appl. Polym. Sci.* **1993**, *48*, 1579−1585. (b) Yamada, K.; Tsutaya, H.; Tatekawa, S.; Hirata, M. *J. Appl. Polym. Sci.* **1992**, *46*, 1065−1085. (c) Bergbreiter, D. E.; Srinivas, B.; Guo-Feng, X.; Aguilar, G.; Ponder, B. C.; Gray, H. N N.; Bandella, A. In *Polymer Surfaces and Interfaces: Characterization, Modification and Application*; Mittal, K. L., Lee, K. W., Eds.; VSP: Utrecht, 1997; pp 3−18.
(21) Berlman, I. B. *Handbook of Fluorescence Spectra of Aromatic Molecules*; 2nd ed.; Academic Press: New York, 1971.
(22) Greenberg, A.; Furst, M.; Kallmann, H. *International Symposium on Luminescence. The Physics and Chemistry of Scintillators*; Verlag Karl Thieme: Munich, 1966.
(23) Cui, C.-X.; Weiss, R. G. *J. Am. Chem. Soc.* **1993**, *115*, 9820−9821.
(24) He, Z.; Jenkins, R. M.; Hammond, G. S.; Weiss, R. G. *J. Phys. Chem.* **1992**, *96*, 496−502.
(25) Naciri, J.; Weiss, R. G. *Macromolecules* **1989**, *22*, 3928−3936.
(26) Cui, C.-X.; Naciri, J.; He, Z.; Jenkins, R. M.; Lu, L.; Hammond, G. S.; Weiss, R. G. *Quim. Nova* **1993**, *16*, 578−585.
(27) Wang, C.; Weiss, R. G. *Macromolecules* **1999**, *32*, 7032−7039.
(28) Jang, Y. T.; Parikh, D.; Phillips, P. H. *J. Polym. Sci.* **1985**, *23*, 2483−2498.
(29) Hendra, P. J.; Passangham, C.; Jones, S. A. *Eur. Polym. J.* **1991**, *27*, 127−134.
(30) Kakizaki, M.; Kakudate, T.; Hideshima, T. *J. Polym. Sci., Polym. Phys. Ed.* **1985**, *23*, 809−924.
(31) Boyer, R. F. *Macromolecules* **1973**, *6*, 288−299.
(32) Boyer, R. F. *J. Macromol. Sci., Phys.* **1973**, *B8*, 503−537.
(33) Goldstein, M. *J. Chem. Phys.* **1969**, *51*, 3728−3739.
(34) McCrum, N. G.; Read, B. E.; Williams, G. *Inelastic and Dielectric Effects in Polymeric Solids*; Wiley: New York, 1967.
(35) Aloisio, C. J.; Matsuoka, S.; Maxwell, B. *J. Polym. Sci., Part A2* **1966**, *4*, 113−119.
(36) Popli, R.; Mandelkern, L. *Polym. Bull. (Berlin)* **1983**, *9*, 260−267.
(37) Glotin, M.; Domszy, R.; Mandelkern, L. *J. Polym. Sci., Polym. Phys. Ed.* **1983**, *21*, 285−294.
(38) Ohta, Y.; Yasuda, H. *J. Polym. Sci., Part B: Polym. Phys.* **1994**, *32*, 2241−2249.
(39) Meakins, R. J. *Prog. Dielectr.* **1961**, *3*, 151−202.
(40) Crissman, J. M.; Passaglia, E. J. *J. Appl. Phys.* **1971**, *42*, 4636−4644.
(41) Crissman, J. M. *J. Polym. Sci., Polym. Phys. Ed.* **1975**, *13*, 1407−1416.
(42) Olf, H. G.; Peterlin, A. *J. Polym. Sci., Part A* **1970**, *8*, 753−770.
(43) Olf, H. G.; Peterlin, A. *J. Polym. Sci., Part A* **1970**, *8*, 771−789.
(44) Buckley, C. P.; McCrum, N. G. *J. Mater. Sci.* **1973**, *8*, 928−940.
(45) Davies, G. R.; Owen, A. J.; Ward, I. M.; Gupta, V. B. *J. Macromol. Sci., Phys.* **1972**, *B6*, 215−228.
(46) Sinnott, K. M. *J. Appl. Phys.* **1966**, *37*, 3385−3400.
(47) Takayanagi, M. *Pure Appl. Chem.* **1967**, *15*, 555−586.
(48) Manabe, S.; Sakoda, A.; Katada, A.; Takayanagi, M. *J. Macromol. Sci., Phys.* **1970**, *B70*, 161−184.
(49) Kajiyama, T.; Okada, T.; Sakoda, A.; Takayanagi, M. *J. Macromol. Sci., Phys.* **1973**, *B7*, 583−608.
(50) Blatt, E.; Treloar, F. E.; Ghiggino, K. P.; Gilbert, R. G. *J. Phys. Chem.* **1981**, *85*, 2810−2816.
(51) Brown, G. O.; Guardala, N. A.; Price, J. L.; Weiss, R. G. *J. Phys. Chem. B* **2002**, *106*, 3375−3382.
(52) Cui, C.-X. Ph.D. Thesis, Georgetown University, Washington, DC, 1995.
(53) Nakaya, T.; Tomomoto, T.; Imoto, M. *Bull. Chem. Soc. Jpn.* **1967**, *40*, 691−692.
(54) Nakaya, T.; Ohashi, K.; Imoto, M. *Makromol. Chem.* **1968**, *111*, 115−122.
(55) Birks, J. B. *Photophysics of Aromatic Molecules*; John Wiley: New York, 1970; pp 71, 521.
(56) Atvars, T. D. Z.; Talhavini, M. *Quim. Nova* **1995**, *18*, 298−300.
(57) Gilbert, A.; Baggot, J. *Essentials of Molecular Photochemistry*; Wiley-Interscience: New York, 1970.
(58) Förster, T. *Discuss. Faraday Soc.* **1959**, *27*, 7−17.
(59) Förster, T. *Ann. Phys.* **1948**, *2*, 55−75.
(60) Wavemetrics, Inc., Lake Oswego, OR.
(61) Martins, T. D.; Yamaki, S. B.; Prado, E. A.; Atvars, T. D. Z. *J. Photochem. Photobiol. A: Chem.* **2003**, *156*, 91−103.
(62) Roedel, M. J. *J. Am. Chem. Soc.* **1953**, *75*, 6110−6112.
(63) Sperati, C. A.; Franta, W. A.; Starkweather, H. W. *J. Am. Chem. Soc.* **1953**, *75*, 6127−6133.
(64) Wignall, G. D.; Londomo, J. D.; Lin, J. S.; Alamo, R. G.; Galante, M. J.; Mandelkern, L. *Macromolecules* **1995**, *28*, 3156−3167.
(65) Billmeyer, F. W. *J. Am. Chem. Soc.* **1953**, *75*, 6118−6122.
(66) Beasley, J. K. *J. Am. Chem. Soc.* **1953**, *75*, 6123−6127.
(67) Raff, R. A. V. *Crystalline Olefin Polymers*; Interscience: New York, 1965; Vol. 1, p 678.
(68) Bryant, W. M. D.; Voter, R. C. *J. Am. Chem. Soc.* **1953**, *75*, 6113−6118.
(69) Nordel IP NDR-3430, Technical Information, Nordel Grade Selection Guide, DuPont Dow Elastomeres, Wilmington, DE.
(70) Dainton, F. S.; Evans, D. M.; Hoare, F. E.; Melia, T. P. *Polymer* **1962**, *3*, 277−285.
(71) Ashcraft, C. R.; Boyd, R. H. *J. Polym. Sci., Polym. Phys. Ed.* **1976**, *14*, 2153−2193.
(72) Boyd, R. H. *J. Chem. Phys.* **1959**, *30*, 1276−1283.
(73) Woodward, A. E.; Crissman, J. M.; Sauer, J. A. *J. Polym. Sci.* **1960**, *44*, 23−34.
(74) Illers, K. H.; Breuer, H. *J. Colloid Sci.* **1963**, *18*, 1−31.
(75) Arai, H.; Kuriyama, I. *Colloid Polym. Sci.* **1976**, *254*, 967−971.
(76) Ramesh, V.; Weiss, R. G. *Macromolecules* **1986**, *19*, 1486−1489.
(77) Israelachvili, J. N. *Intermolecular & Surface Forces*, 2nd ed.; Academic Press: San Diego, 1992.
(78) By X-ray diffraction.[78a] A previously reported value from DSC was 31%.[13] Brown, G. O., unpublished results.
(79) Coltro, L.; Dibbern-Brunelli, D.; Elias, C. A. B.; Talhavini, M.; de Oliveira, M. G.; Atvars, T. D. Z. *J. Braz. Chem. Soc.* **1995**, *6*, 127−133.

MA034130E